Dynamic, Time-Resolved CT Imaging of Myocardial Perfusion: 320-Slice CT

Narinder S. Paul

Contents

Abstract

Cardiac Computed Tomography has progressed beyond providing a purely detailed anatomical description of coronary disease, to a comprehensive demonstration of anatomic-physiological disturbance that forms the basis of a "one stop shop" for assessment of coronary disease. The 320MDCT wide area detector provides a unique capability to assess the whole heart during a single gantry rotation. This chapter outlines the scientific advances made using the 320MDCT: in animal models of cardiac ischemia followed by translational work in human subjects; initially with discussion of single centre trials followed by introduction of the Core 320 multi-centre trial.

1 Introduction

Computed tomography coronary angiography (CTCA) provides an accurate and non-invasive imaging tool for exclusion of significant coronary artery disease (CAD). However, the presence of arterial disease on CTCA correlates poorly with perfusion abnormalities noted on myocardial perfusion imaging (MPI) (Hacker et al. 2005; Schuijf et al. 2006; Klocke et al. 2003). Myocardial perfusion imaging (MPI) lacks the anatomical resolution of CTCA for coronary disease but is established as a useful tool in the diagnosis and prognosis of patients with CAD (Klocke et al. 2003). Therefore there has been considerable interest in providing a "one stop" comprehensive cardiac assessment with computed tomography (CT) by combining the high spatial resolution images of coronary artery anatomy provided by CTCA with myocardial perfusion indices from CT perfusion (CTP). As dipyridamole or adenosine induced coronary vasodilatation has been demonstrated to provide equivalent cardiac stress as compared to exercise stress testing with single-photon emission tomography

N. S. Paul (✉)
Joint Department of Medical Imaging
and the Peter Munk Cardiac Centre,
Toronto General Hospital, University of Toronto,
Toronto, Canada
e-mail: narinder.paul@uhn.on.ca

U. J. Schoepf et al. (eds.), *CT Imaging of Myocardial Perfusion and Viability*, Medical Radiology. Diagnostic Imaging,
DOI: 10.1007/174_2012_792, © Springer-Verlag Berlin Heidelberg 2013
Published Online: 17 January 2013

(SPECT) in diagnosing CAD (Nguyen et al. 1990; Parodi et al. 1991; Coyne et al. 1991; Nishimura et al. 1992; Gupta et al. 1992), these agents have been incorporated into CTP protocols.

The purpose of this chapter is to highlight advances in myocardial perfusion and viability imaging using the Aquilion CT series (Toshiba Medical Systems, Otawara, Japan) culminating in the Aquilion ONE, 320 multi detector row computed tomography (320MDCT) scan unit.

CT perfusion image acquisition is performed during first pass myocardial perfusion of iodinated contrast medium (CM) through the blood pool and the left ventricular (LV) myocardium. Regions of interest (ROIs) are prescribed in the blood pool and LV myocardium to create time attenuation curves (TACs) from which the myocardial blood flow (MBF) can be calculated. Accurate data analysis relies on the validity of several assumptions including: (1) there is complete mixing of the iodinated contrast with the blood before it arrives in the heart, (2) there is minimal recirculation of the iodinated contrast, (3) the measured CT attenuation number (in Hounsfield Unit, HU) accurately corresponds to the concentration of the iodinated contrast, (4) the volume of iodinated contrast is negligible compared to the blood volume, (5) the iodinated contrast does not induce physiologic or hemodynamic changes during cardiac transit, and (6) the iodinated contrast remains within the intravascular compartment during first pass perfusion (Rumberger and Bell 1992; Rumberger et al. 1987).

An initial investigation into myocardial viability assessment by computer tomography was performed using 32MDCT in canine and porcine models (Lardo et al. 2006). Ten anesthetised and mechanically ventilated canines had induced occlusion of the proximal left anterior descending (LAD) coronary artery by inflating a 3-mm angioplasty balloon for 90 min. Quantification of MBF was performed by measurement of injected neutron activated microspheres into the LV cavity before, during, and after LAD occlusion. Cardiac CT was administered, the animals were sacrificed, and post mortem analysis was performed. Similarly, LAD occlusion was performed in seven anesthetised and mechanically ventilated pigs that had inflation of a 3-mm balloon in the mid LAD for 60 min. The animals recovered for 8 weeks and then had cardiac CT performed under sedation. The pigs were subsequently sacrificed and post mortem analysis was performed. Cardiac CT was performed using a detector collimation of 32 × 0.5 mm, tube potential of 135 kV, tube current of 420 mA, gantry rotation of 400 ms, and a pitch of 7.2. The heart rate was controlled to less than 100 bpm by using 2–5 mg of intravenous propranolol, and post infarct arrhythmias were suppressed by using intravenous lidocaine. A 150 mL bolus of intravenous CM containing 320 $mg{\cdot}mL^{-1}$ iodine was injected and image acquisition was triggered at a density threshold of 150 HU in the ascending aorta. Retrospectively gated cardiac imaging was performed at first pass and every 5 min for 40 min. Axial 0.5-mm images were reconstructed at 75 % of the R–R interval with additional image reconstructions for functional analysis. Image analysis was performed with proprietary cardiac software (Toshiba Medical Systems) that performed automated border detection with delineation of endocardial and epicardial borders. Qualitative and quantitative analysis revealed peak myocardial attenuation at 5 min following injection of CM with decrease in attenuation over 40 min. Areas of hyper- and hypo-attenuation were manually traced and represented infarcted myocardium and areas of microvascular obstruction respectively. The MDCT assessment of infarct size and depth correlated well with post mortem assessment. This study demonstrated that 32MDCT can accurately determine myocardial viability by delineating and characterising acute and chronic myocardial infarction.

Early validation of first-pass, contrast-enhanced helical 64MDCT imaging was used to detect a myocardial flow deficit due to an induced stenosis in the left anterior descending (LAD) coronary artery during adenosine stress imaging (George et al. 2006). The research was performed using a canine model in which a 50 % LAD artery stenosis was induced. Baseline and post-stress MBF were measured using neutron-activated microspheres that were injected into the left atrium and sampled in the descending thoracic aorta. Intravenous propranolol (5–20 mg) was used to maintain a heart rate below 100 bpm. Intravenous adenosine was infused for 5 min at 140–210 $mcg{\cdot}kg^{-1}{\cdot}min^{-1}$. Intravenous CM containing 320 mg $iodine{\cdot}mL^{-1}$ was injected at 2.5 $mL{\cdot}s^{-1}$ for 40 s. Automated threshold-triggered image acquisition was initiated at a density threshold of 180 HU in the descending thoracic aorta using retrospective ECG gating, detector collimation of 32 × 0.5 mm, tube potential of 120 kV, tube current of 400 mA, a gantry rotation of 400 ms, and a helical pitch 6.4–8.8. Segmented image reconstruction was performed at 10 % phase intervals of the acquired R–R cycle. The 80 % phase was chosen for image reconstruction and 4-mm LV short axis images were reconstructed. ROIs were located through LV wall segments in the LAD territory and remote myocardium. Measurement values from the remote myocardium were used to define the mean and standard deviation (SD) of attenuation (in HU) for normal-perfused myocardium. Therefore, under-perfused myocardium was defined as one SD below this threshold. The results in seven canine models demonstrated significant differences in qualitative assessment and semi-quantitative assessment of perfused (180.4 ± 41.9 HU) and under-perfused (92.3 ± 39.5 HU) myocardium. Calculations of flow reserve in perfused (7.3 ± 4.7) and under-perfused (0.17 ± 0.07) myocardium also showed significant differences. This study demonstrated that first-pass, contrast-enhanced helical

64MDCT imaging can detect significant LAD territory flow disturbance using adenosine stress; and that MDCT derived parameters of LV myocardial perfusion have good correlation with microsphere-derived absolute MBF.

Subsequent research prompted evaluation of myocardial perfusion with dynamic CTP in six canines with induced 50 % LAD stenosis (George et al. 2007). Image acquisition relied on a stationary table during gantry rotation and injection of iodinated contrast material (CM) in order to record changes in tissue attenuation over time. This allowed TAC to be plotted and enabled quantification of absolute MBF.

Each canine was positioned such that the mid to distal LV was in the scan plane. Intravenous adenosine (140 mcg·kg^{-1}·min^{-1}) was infused for 5 min followed by 30 mL of intravenous CM containing 320 mg iodine·mL^{-1} injected at 10 mL·s^{-1}. Image acquisition occurred using a detector collimation of 8 mm × 4 mm, tube potential of 120 kV, tube current of 150 mA, a gantry rotation time of 400 ms, and a scan time of 70 s. Intravenous metoprolol (5–20 mg) was used to maintain a heart rate below 100 bpm; respiratory motion was suppressed using pancuronium (0.1 mg·kg^{-1}). The MBF was measured during adenosine infusion, by injecting neutron-activated microspheres into the left atrium and performing quantitative measurements in the proximal descending aorta. Short-axis images through the LV were reconstructed using 8 mm slice thickness and ROIs were located through the target anterior LV wall and the remote inferior and lateral walls to create TAC. The TAC was normalised for the arterial input function (AIF) by using the ratio of the LV blood pool upslope to the LV blood pool peak enhancement. A dual compartment deconvolution method was applied to the myocardial upslope-to-LV-upslope and myocardial upslope-to-LV-max ratio to evaluate dynamic MDCT myocardial perfusion. This analysis demonstrated a strong correlation between the semi-quantitative CT imaging results and the microsphere MBF measurements. This study confirmed the accuracy of 64MDCT perfusion using the myocardial upslope normalized to the LV blood pool upslope or the maximum LV attenuation density, and also the application of model-based deconvolution analysis to dynamic MDCT TAC.

Although dynamic CTP analysis was shown to be accurate for myocardial perfusion, the limited scan coverage with 64MDCT required adaptation of the technique with helical acquisition for whole-LV assessment. The next stage in evolution of CTP utilized a combination of dynamic image acquisition; incorporating images acquired during bolus tracking to acquire the AIF curve together with ECG-gated helical acquisition of the entire LV myocardium (George et al. 2010). The technique was initially validated in four healthy canines scanned on 64MDCT using bolus tracking and a helical scan mode during injection of iodinated (320 mg iodine·mL^{-1}) CM at 4 mL·s^{-1} using a triphasic protocol: an initial 16 mL of 100 % CM followed by 40 mL of 30 % CM–70 % normal saline mixture, and a final 50 cc of 100 % normal saline. A retrospective ECG-gated acquisition was used with 64 × 0.5 mm detector collimation, 120 kV tube potential, 400 mA tube current, 400 ms gantry rotation time, and a helical pitch of 14.4–16.2. The bolus tracking data were reconstructed at 400 ms intervals using a 2 mm slice thickness, ROIs were prescribed in the aortic root to create the TAC for the early part of the AIF. Helical images were then reconstructed at 80 % of the R–R interval using a 4 mm slice thickness and a ROI prescribed in the intravascular blood pool from the aortic root through the LV outflow tract to the LV apex. The signal intensity of the blood pool was correlated with the time of image acquisition for the axial slices and the data used to construct the latter part of the TAC of the AIF. The TAC was adjusted for baseline attenuation. After a washout period of 10 min, the canine hearts were re-scanned during injection of iodinated intravenous CM; a dynamic MDCT scan was performed for 60 s through the aortic root using the same X-ray tube exposure parameters as for the helical scan with and a detector collimation of 4 × 8 mm. Images were reconstructed at 8 mm slice thickness and 400 ms intervals. A ROI was prescribed in the aortic root and plotted against time for a TAC. Data values were corrected for baseline attenuation. The bolus tracking and helical acquisitions were repeated in seven canines that had induced LAD stenosis. Neutron activated microspheres were injected following the helical acquisition and sampled in the descending thoracic aorta in order to measure the myocardial blood flow. The AIF was calculated from the bolus tracking and helical acquisitions and myocardial perfusion was measured in the left ventricle. This study demonstrated that the early and late phases of the TAC of the AIV could be calculated using available data from the automated bolus tracking threshold trigger in cardiac CT and that the helically acquired MDCT images had good correlation with microsphere generated indices of MBF ($R2 = 0.86$, $P < 0.001$).

Increased appreciation of LV myocardial blood flow, specifically the differential blood supply to the LV wall with increased perfusion to the subendocardium compared with the subepicardial segments, created interest in evaluation of a transmural perfusion ratio (TPR) (George et al. 2009). In this study, 40 patients with documented abnormal SPECT MPI had CTCA and CTP within 60 days. Patients were randomized to stress/perfusion cardiac CT with either 64MDCT or with 256MDCT. All patients received similar preparation with oral/intravenous metoprolol to maintain a heart rate below 65 bpm and intravenous hydration with 250–500 mL normal saline. All patients had an infusion of

intravenous adenosine (140 mcg·kg^{-1}·min^{-1}) for 5 min prior to injection of 90–95 mL of CM containing 370 mg·mL^{-1} iodine injected at 5 mL·s^{-1} followed by 30 mL of normal saline. Patients scanned with 64MDCT had image acquisition triggered automatically at a threshold of 150 HU in the LV blood pool. The retrospectively ECG-gated acquisition was performed using 64 × 0.5 mm detector collimation, tube potential of 120 kVp, tube current of 400 mA, gantry rotation of 400 ms, and a pitch that varied with heart rate. Images were obtained for a combined stress CTCA-CTP study. Patients scanned with 256MDCT had an initial test bolus injection of 20 mL CM (370 mg iodine mL^{-1}) at 5 mL·s^{-1} to determine peak arterial enhancement. For CTP imaging, a triphasic intravenous protocol was used at 5 mL·s^{-1}: 50 mL of 100 % contrast (370 mg iodine mL^{-1}), 20 mL of 50 % contrast and saline, and 30 mL normal saline. The detector collimation was 128 × 1.0 mm, tube potential was 120 kV, tube current was 200 mA, gantry rotation was 500 ms, and scan time was 1.5 s. A 10-min rest/wash-out period was required after acquisition of the stress CTP images prior to a second injection of 60 mL iodinated CM at 5 mL·s^{-1} to obtain a diagnostic CTCA and rest perfusion images using a detector collimation of 256 × 0.5 mm, a tube potential of 120 kV, a tube current of 350 mA, a gantry rotation of 500 ms, and a scan time 1.5 s. Cardiac perfusion analysis was performed for all patients using contiguous 3-mm images orientated in the short axis of the left ventricle from end diastolic phases (80–100 % R–R) by using an automated border detection algorithm to define the subendocardial, mid-myocardial, and subepicardial borders in a 16-segment LV anatomical perfusion model. The TPR was defined as the attenuation ratio of the subendocardium to the subepicardium and was calculated separately for each segment. Invasive catheter coronary angiography and quantitative coronary analysis were performed in 27 patients. In patients without CAD, the mean TPR was 1.12 ± 0.13 with good interobserver variability for rest ($\kappa = 0.72$, 95 % CI, 0.63–0.802) and stress ($\kappa = 0.63$, 95 % CI, 0.56–0.70) images. The TPR decreased with increasing luminal stenosis and measured 1.09 ± 0.11 for 30–49 % stenosis, 1.06 ± 0.14 for a 50–69 % stenosis, and 10.91 ± 0.10 for a high grade stenosis (≥70 %). This study demonstrated a significant inverse relationship between the TPR and the severity of luminal stenosis.

Increased experience of CTP analysis reinforced the importance of standardising image assessment in order to understand the range of normal appearances and to minimise misinterpretation of artifacts. For qualitative image analysis, a narrow window (W200–300) and level setting (L100–150) is recommended for stress, rest, and delayed enhancement images (Ko et al. 2011). Typical values of attenuation for non-enhanced myocardium ranges from 40

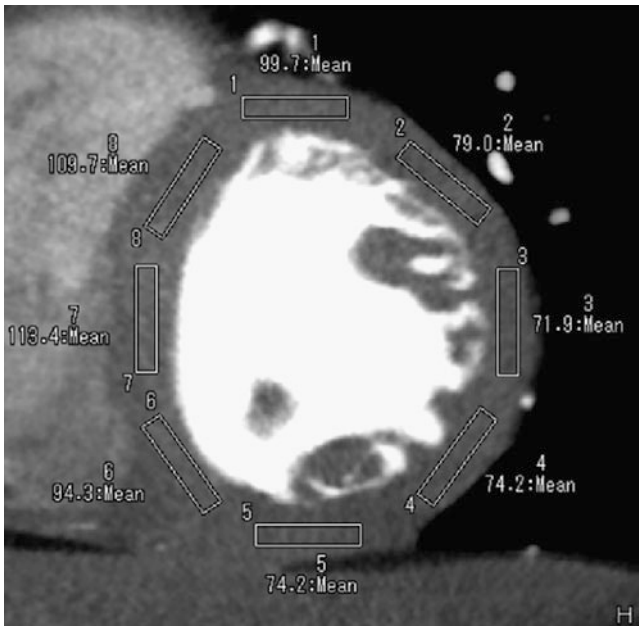

Fig. 1 Short-axis reconstruction through the left ventricle illustrating locations of ROI and corresponding LV myocardium attenuation values (in HU)

to 60 HU, and normal myocardium enhances from 100 to 120 HU (Valdiviezo 2010). The regional distribution of LV wall enhancement was evaluated in consecutive patients who had cardiac CT performed using 320MDCT without vasodilator stress (Crossett et al. 2011). Image acquisition was performed using a detector collimation of 240–320 × 0.5 mm, a tube potential of 100–135 kV, a tube current of 400–580 mA, a gantry rotation of 350 ms, and a temporal exposure window of 70–80 % of the R–R interval. Oral metoprolol (50–100 mg) with supplementary intravenous metoprolol (5–30 mg) was administered to maintain a heart rate below 65 bpm. Sublingual nitrates (40 mcg) were given followed by a dual phase injection of iodinated CM containing 350 mg·mL^{-1} iodine with an initial bolus of 75 mL at 6 mL·s^{-1} followed by 50 mL of normal saline at the same rate. Image acquisition was triggered at a threshold of 300 HU in the descending thoracic aorta. Twenty-one patients had normal epicardial arteries. In these patients, 5-mm thick short axis images were reconstructed through the left ventricle at basal, mid, and apical regions. Eight identical rectangular ROIs were placed in the mid myocardium, covering all segments but not restricted to the American Heart Association 17-segment model (Fig. 1).

Analysis of the LV myocardium enhancement demonstrated that the lateral myocardial LV wall has a mean attenuation of 79.4 HU (42.3–162.7 HU) in the mid ventricle compared with the inferior, septal, and anterior LV wall segments at this level, which demonstrate a mean attenuation of 103.9 HU (11.4–159.6 HU). This study suggested that there is differential enhancement of the left

ventricle myocardium at rest in patients with normal epicardial coronary arteries as demonstrated on 320MDCT.

Assessment of CTP using 320MDCT and vasodilator stress was performed in a cohort of patients without documented CAD (Kühl et al. 2012). This prospective study recruited healthy subjects to one of three groups, each with 14 subjects as follows: group 1a had MPI at rest using ^{13}NH3–PET, group 1b had rest CTCA–CTP, and group 2 had rest CTCA–CTP and stress CTP using adenosine infusion at 140 mcg·mL^{-1}·min^{-1}. LV analysis was performed using a 16-segment AHA model (apex excluded). The myocardium was divided into three layers: the sub-endocardium, the mid-myocardium, and the sub-epicardium; the relative TPR was calculated for each segment. The results confirmed the differential segmental perfusion of the LV myocardium that had been previously demonstrated on CTP; the highest values were measured in anteroseptal segments, 1, 2, 3, 7, 8, 9, while the lowest values were observed in the lateral wall in segments, 5, 6, 11, 12, and 16. This pattern of perfusion was mirrored by ^{13}NH3–PET. At rest, sub-endocardial perfusion was higher than for the mid-myocardium and the sub-epicardium. With vasodilator stress, there was a 21 and 23 % increase in perfusion to the mid-myocardium and the sub-epicardium, respectively, which eliminated any significant density gradient between these layers. Similarly, the overall increase in myocardial perfusion due to vasodilator stress also led to a significant reduction in segmental variation of relative perfusion values. This study demonstrated that segmental differences in LV myocardium perfusion seen with 320MDCT in healthy subjects are mirrored using ^{13}NH3–PET imaging and that this may be a true physiological phenomenon rather than artifact. In addition, vasodilator stress significantly increases overall myocardial perfusion and decreases the segmental and transmural variation in LV perfusion.

However, motion and beam hardening artifacts can influence the relationship between the measured CT attenuation number and concentration of iodinated contrast (Mehra et al. 2011a, b). Motion artifact are minimized through the use of beta blockers during combined CTCA and CTP protocols. Beam hardening artifacts occur when there is preferential absorption of low-kV photons as the X-ray beam passes through the iodinated CM. The resulting higher energy emergent X-ray beam produces beam-hardening artifacts which simulate perfusion defects in the LV myocardium (Brooks and Di Chiro 1976; Zatz and Alvarez 1977).

The characteristics of beam hardening artifacts were evaluated in a phantom study using the 320MDCT (Kitagawa et al. 2010). An anthropomorphic LV urethane phantom was constructed with and without lesions that simulated perfusion defects that measured 50 % of the LV wall thickness in depth and 90 ° in circumference. An 18-mm syringe simulated the thoracic aorta and both were placed in an anthropomorphic chest phantom, which had water bags placed within the thoracic cavity and around the chest phantom. The phantom was scanned with a 320MDCT unit using the following imaging protocol: collimation of 320 × 0.5 mm, tube voltage of 120 kV, tube current of 500 mA, and gantry rotation time of 350 ms. Half-reconstruction 3-mm thick images orientated along the LV short axis were reconstructed using a standard body kernel, FC13, without beam hardening correction (BHC); another set of images were reconstructed using the standard body kernel, FC03, but with BHC. The LV cavity and syringe were filled with water, scanned, and then filled with iodinated CM and re-scanned. The BHC correction algorithm compared the degree of beam hardening from areas of high contrast (iodinated contrast) to those from areas of water density in order to produce a corrected image (Olson et al. 1981). The attenuation of the "normal" perfused myocardium was measured without BHC. Beam hardening was defined if the measured attenuation was less than 2 SD of this value. The algorithm was then tested in a canine model with an induced 50 % reduction in hyperaemic flow either in the LAD or left circumflex (Cx) coronary arteries. The animal was placed in a 256MDCT such that the scan range covered the entire heart. Intravenous metoprolol (5–30 mg) was given to achieve a heart rate below 100 bpm and pancuronium (0.1 mg·kg^{-1}) to minimise respiratory motion artifacts. An infusion of intravenous adenosine (0.14 mg·kg^{-1}·min^{-1}) was given over 5 min during which time intravenous CM containing 370 mg iodine·mL^{-1} was injected at 4 cc·s^{-1} for 6 s. Image acquisition was performed using a dynamic volume CT scan mode with a detector collimation of 256 × 0.5 mm, a gantry rotation time of 500 ms, tube potential of 120 kV, tube current of 100 mA, and a scan time of 60 s. Short axis 0.5 mm images were created through the mid ventricle using a mid-diastolic phase and multi-segmented reconstruction, with and without BHC. ROIs were drawn in the LV wall and in the left and right ventricular cavities; TACs were calculated for each ROI. Upslope analysis was performed by comparing the TAC for the LV blood pool to the peak enhancement in myocardium, normalized by the peak LV blood pool enhancement. Assessment of MBF was compared with injected microspheres. The phantom data confirmed that beam hardening artifacts interfered with the demonstration of perfusion defects. However, the BHC algorithm effectively improved the demonstration of the true defects and accounted for the presence of iodinated CM in the LV cavity and descending thoracic aorta. The BHC had a variable influence on improving the upslope perfusion analysis in the canine model with an unpredictable performance in the interventricular septum. This study demonstrated that beam hardening artifact is an important confounder in CT assessment of myocardial perfusion and that it can be partially corrected in vivo using a BHC algorithm.

Table 1 Per vessel territory diagnostic accuracy of computed tomography coronary angiography, computed tomography myocardial perfusion imaging, and quantitative coronary angiography compared with fractional flow reserve (n = 86)

	CTA DS≥50%	Perfusion defect on CTP	CTA DS ≥50 % and perfusion defect on CTP	CTA DS ≥50 % or perfusiondefect on CTP	QCA DS≥50 %	QCA DS≥70%
True positive (n)	38	31	28	41	29	11
False positive (n)	18	7	1	24	17	1
True negative (n)	27	38	44	21	28	44
False negative (n)	3	10	13	0	12	30
Sensitivity (%)	93 (84–100)	76 (62–89)	68 (54–83)	100 (89–00)	71 (55–87)	27 (12–41)
Specificity (%)	60 (43–77)	84 (73–96)	98 (93–100)	47 (31–63)	62 (47–78)	98 (93–100)
PPV (%)	68 (53–82)	82 (67–96)	97 (89–100)	63 (49–77)	63 (46–80)	92 (72–100)
NPV (%)	90 (79–100)	79 (65–93)	77 (64–90)	100 (81–100)	70 (54–86)	59 (48–71)
Kappa statistic	0.52 (0.35–0.69)	0.60 (0.43–0.77)	0.67 (0.52–0.82)	0.52 (0.37–0.68)	0.33 (0.13–0.53)	0.25 (0.10–0.40)
Accuracy (%)	76	80	84	73	66	64

Intracoronary pressure-derived fractional flow reserve (FFR) is the clinical gold standard for assessing the need for revascularization of a discovered coronary artery stenosis (Pijls et al. 1996). The utility of CTP and combination CTCA/CTP with 320MDCT for evaluating patients under consideration for revascularization was compared with FFR in 42 patients who presented with chest pain and had greater than 50 % luminal stenosis on coronary angiography (Ko et al. 2012). All patients had FFR, CTA, CTP, and delayed contrast enhanced cardiac CT within 14 days of the catheter coronary angiography. Of this study cohort, 31 out of 42 (74 %) patients had perfusion abnormalities on CTP, 22 patients (52 %) had a single-vessel territory perfusion defect and 9 (21 %) had two-vessel territory perfusion defects. The majority (60 %) of perfusion defects were located in the LAD territory. All perfusion defects on CTP were reversible. FFR was performed in 68 % of all vessels and when compared with CTA, CTA had a sensitivity, specificity, PPV, and NPV of 93, 60, 68, and 90 % for significant coronary artery disease. In comparison with FFR, CTP had the following performance; sensitivity 76 %, specificity 84 %, PPV 82 %, and NPV 79 %. The combination of a stenosis ≥50 % on CTA and a perfusion defect on CTP had a sensitivity of 68 %, NPV 77 %, specificity 98 %, and PPV of 97 %. These results are illustrated in Table 1.

Interestingly, the combination of stenosis greater than 50 % on CTCA and a corresponding perfusion defect on CTP had 84 % accuracy for predicting ischemia, whereas a stenosis of greater than 50 % on CTA without a perfusion defect had 100 % accuracy for excluding a significant stenosis. The combination of CTCA and CTP was superior to QCA in predicting the need for coronary revascularization. However, discordant findings remained problematic as 37 % of vessels with a normal CTP and greater than 50 % stenosis on CTCA were above the ischemic threshold on FFR, and 67 % of vessels with greater than 50 % stenosis on CTCA and a perfusion defect had normal FFR. The likely explanation for the false positive CTP results was beam hardening or motion artifacts; false negative findings were likely due to a small perfusion defect or motion artifact.

As the majority of patients referred for assessment of CAD will initially have non-invasive cardiac imaging under physiological stress, and in most cases this will be single photon emission computed tomography (SPECT MPI), there is increased interest in comparing the performance of CTCA and CTP against SPECT–MPI. A prospective study of 50 patients (36 males) with intermediate-to-high pre-test probability for CAD and a clinically indicated SPECT–MPI had a research 320MDCT scan performed within 60 days (George et al. 2012). Patients with a heart rate above 65 bpm were given oral or intravenous metoprolol. All patients were given

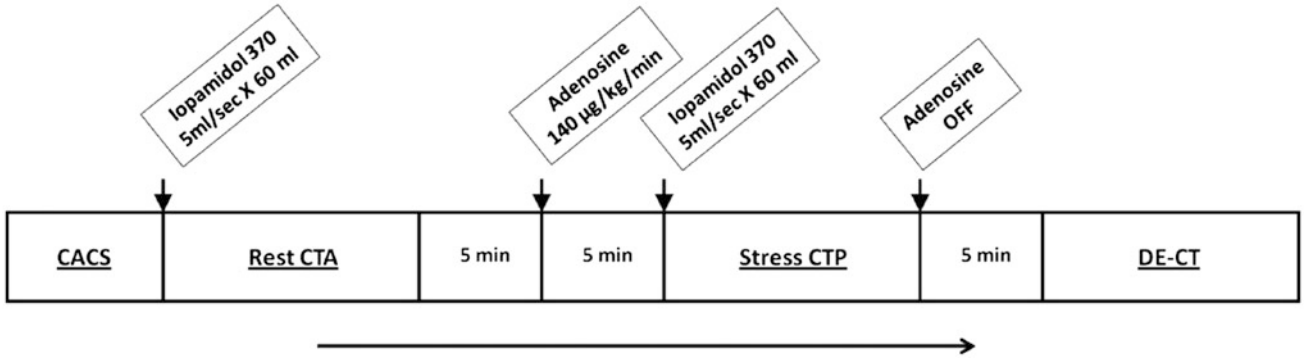

Fig. 2 Outline of a comprehensive cardiac computed tomography (CT) protocol for coronary artery calcium scoring (CACS), rest CT angiography and perfusion (CTA), stress CT perfusion (CTP), and delayed enhanced CT (DECT)

Table 2 Diagnostic accuracy of myocardial computed tomography perfusion and coronary computed tomography angiography (using >50 and >70 % diameter stenosis thresholds) to diagnose reversible ischemia compared with the reference standard single photon emission computed tomography myocardial perfusion imaging

	CTP versus SPECT	CTA Stenosis ≥50 % versus SPECT	CTA Stenosis ≥70 % versus SPECT
Per patient analysis versus SPECT			
Sensitivity	72 (46–89) 13/18	56 (31–78) 10/18	39 (18–64) 7/18
Specificity	91 (74–98) 29/32	75 (56–88) 24/32	91 (74–98) 29/32
PPV	81 (54–95) 13/16	56 (31–78) 10/18	70 (35–92) 7/10
NPV	85 (68–94) 29/34	75 (56–88) 24/32	73 (56–85) 29/40
AUC	0.81 (0.68–0.91) $P < 0.001$	0.65 (0.51–0.78) $P = 0.07$	0.65 (0.50–0.78) $P = 0.08$
Per vessel analysis vs SPECT			
Sensitivity	50 (32–68) 16/32,	25 (12–44) 8/32	22 (10–40) 7/32
Specificity	89 (82–94) 105/118	85 (77–90) 100/118	96 (90–98) 113/118
PPV	55 (35–73) 16/29	31 (15–52) 8/26	58 (29–84) 7/12
NPV	87 (79–92) 105/121	81 (72–87) 100/124	82 (74–88) 113/138
AUC	0.70 (0.62–0.77) $P < 0.001$	0.55 (0.47–0.63) $P = 0.40$	59 (0.51–0.67) $P = 0.13$

SPECT indicates single photon emission computed tomography
CTP computed tomography myocardial perfusion imaging
CTA computed tomography coronary angiography
PPV positive predictive value
NPV negative predictive value
AUC area under the receiver operator characteristic curve

intravenous hydration with 250–500 mL normal saline. The protocol is shown in Fig. 2.

Analysis of rest and stress CTP were performed on a dedicated workstation (Myoperfusion, Toshiba Medical Systems, Otawara, Japan). 3 mm short axis images through the LV were analyzed using a 16-segment model (apex excluded) and by dividing the LV wall into the subendocardium, mid-myocardium, and subepicardium. The mean attenuation of each myocardial layer for each segment was calculated. The ratio of the subendocardial attenuation to the subepicardial attenuation for each segment was calculated to represent the transmural perfusion ratio (TPR). A ratio of less than 0.99 was recorded as abnormal. Coronary CTA analysis was performed using a 19-segment model for vessels larger than 1.5 mm in diameter; uninterpretable segments were excluded from analysis. A luminal stenosis over 50 % was taken as abnormal with a secondary analysis based on luminal stenosis greater than 70 %. 19 patients had coronary angiography. The mean Agatston score was 170 ± 281 (0–1148), CTCA

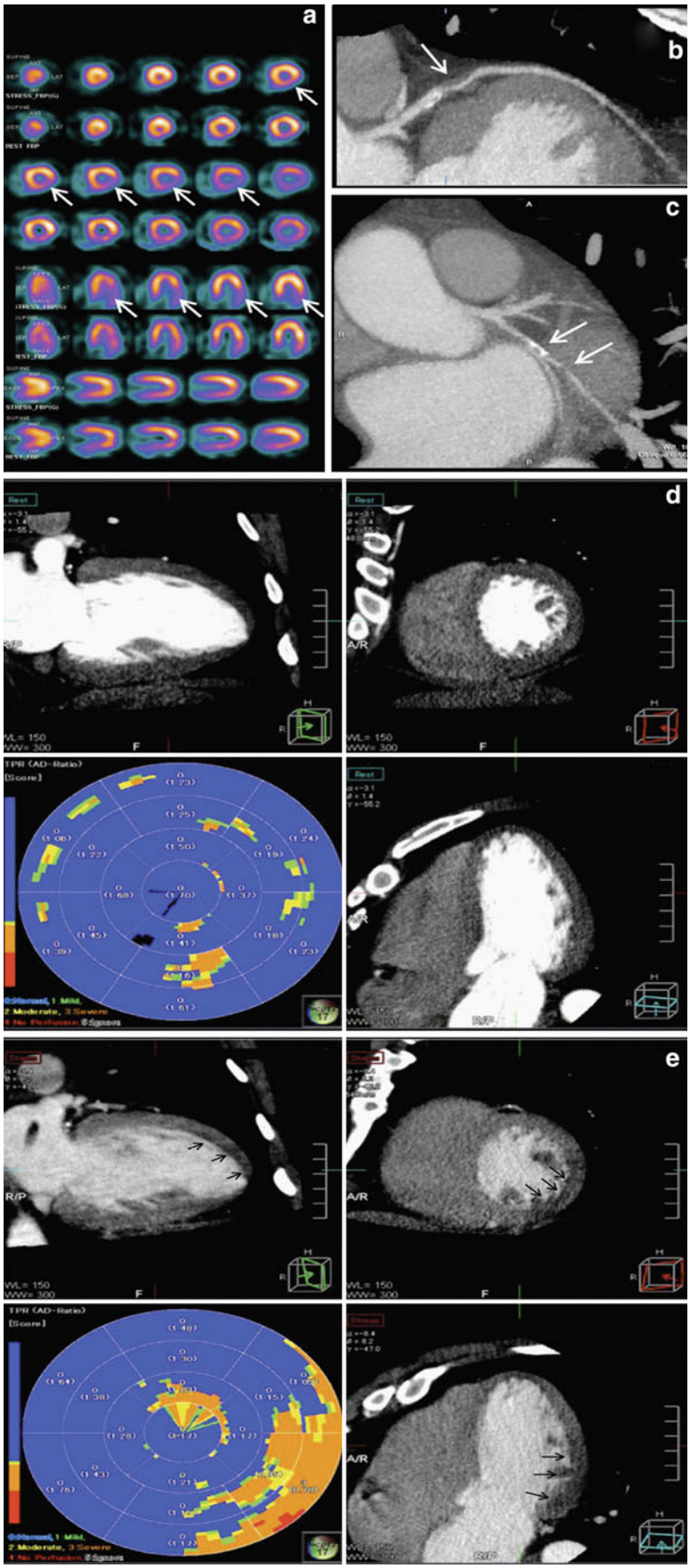

Fig. 3 55-year-old with exertional chest pressure. **a** Short axis, horizontal, and vertical long axis myocardial perfusion images from single photon emission computed tomography demonstrating a reversible perfusion deficit in the basal to midinferolateral wall consistent with myocardial ischemia (*white arrows*). **b** and **c** An intermediate severity stenosis (50–69%) in the mid LAD artery and a severe stenoses in the left circumflex (70–99%) and obtuse marginal branch (70–99%; *white arrows*). **d** The quantitative analysis of rest computed tomography perfusion (CTP) using a 16-segment polar plot, with *blue* representing normal perfusion (transmural perfusion ratio [TPR]_0.99). **e** Adenosine stress CTP. The 16-segment polar plot and images demonstrate abnormal perfusion in the inferolateral and distal anterior wall (*white arrow*). Abnormal TPR (_0.99) is displayed in *yellow*, *orange*, and *red*

Table 3 Diagnostic accuracy of myocardial computed tomography perfusion to diagnose reversible ischemia in the presence of obstructive atherosclerosis (using >50 % and >70 %) diameter stenosis thresholds

	CTP versus CTA Stenosis ≥50 % + SPECT	CTP versus CTA Stenosis ≥70 % + SPECT
Per patient analysis versus CTA/SPECT		
Sensitivity	100 (60–100) 8/8	100 (56–100) 7/7
Specificity	81 (65–91) 34/42	79 (64–89) 34/43
PPV	50 (26–74) 8/16	44 (21–69) 7/16
NPV	100 (87–100) 34/34	100 (87–100) 34/34
AUC	0.91 (0.79–0.97) $P < 0.001$	0.90 (0.78–0.96) $P < 0.001$
Per vessel analysis versus CTA/SPECT		
	Sensitivity 100 (60–100) 8/8	100 (56–100) 7/7
Specificity	85 (78–90) 121/142	85 (77–90) 120/142
PPV	28 (13–47) 8/29	25 (11–44) 7/28
NPV	100 (96–100) 121/121	100 (96–100) 121/121
AUC	0.93 (0.87–0.96) $P < 0.001$	0.92 (0.87–0.96) $P < 0.001$

CTA indicates computed tomography coronary angiography
SPECT single photon emission computed tomography
CTP computed tomography myocardial perfusion imaging
PPV positive predictive value
NPV negative predictive value
AUC area under the receiver operator characteristic curve

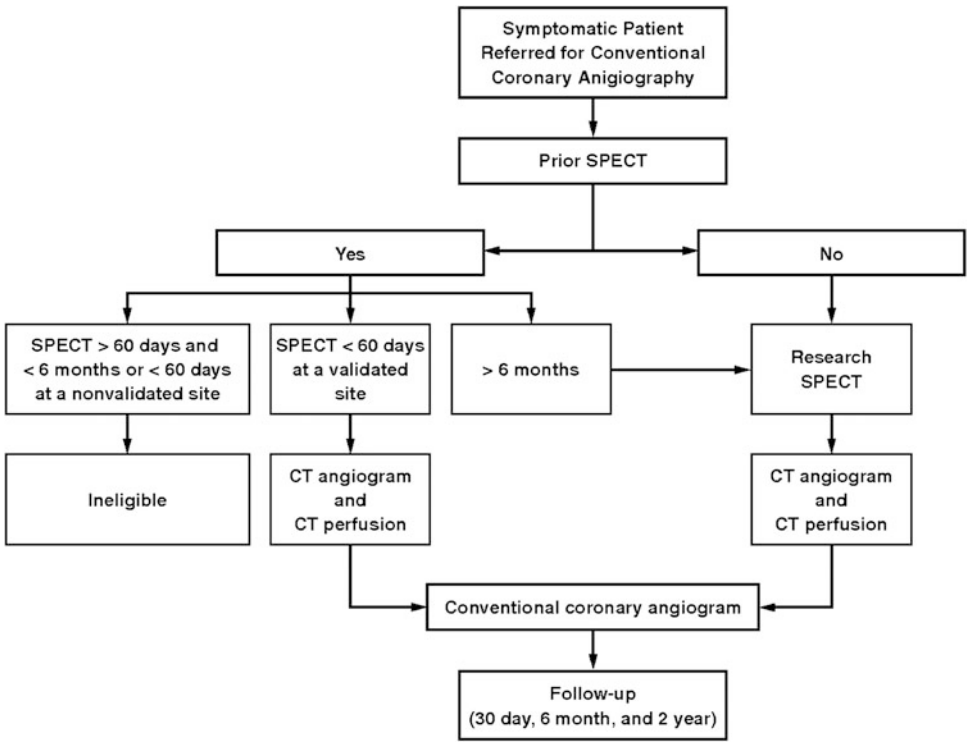

Fig. 4 Overall enrollment strategy of CORE320 Multicenter study. All patients enrolled with clinical indication for invasive coronary angiography will undergo either clinical or research SPECT study at validated site, MDCT angiography and perfusion study, and invasive coronary angiography within 60 days of each other

demonstrated luminal stenosis greater than 50 % in 18 out of 50 (36 %) patients and greater than 70 % stenosis in 10 out of 50 (20 %) patients. CT perfusion (CTP) demonstrated perfusion abnormalities in 36 % (18 out of 50) patients and 21 % (32 out of 150) vascular territories, 75 % (24 out of 32) of which were reversible defects and 22 % (7 out of 32) were partially reversible. Figure 3 illustrates a case example of perfusion defects seen on 320MDCT.

The sensitivity, specificity, PPV, NPV, and AUC for 50 %-lesions on CTCA to predict a perfusion deficit on SPECT–MPI was 56, 75, 56, 75, and 0.65 %, respectively. The corresponding values for lesions constituting greater than 70 % luminal stenosis on CTCA were 39, 91, 70, 73, and 0.65 % (Table 2).

Using CTP in isolation, the sensitivity, specificity, PPV, NPV, and AUC improved to 72, 91, 81, 85, and 0.81 %, respectively; when CTP was compared to a combination of CTCA and SPECT, there was a significant improvement in performance characteristics (Table 3).

The study was limited with a suboptimal per-vessel sensitivity of CTP compared with SPECT, it was theorized that this could be due to false-positive SPECT studies or inaccuracies in TPR analysis due to motion, beam hardening, and reconstruction artifacts, all of which could result in underestimating the presence of ischemia. The total radiation dose from the calcium score (CACS), rest, stress, and delayed cardiac CT was 13.8 ± 2.9 mSv, comparable to that for a rest-stress MPI 13.1 ± 1.7 mSv. This study demonstrated the utility of 320MDCT to perform combined CT angiography and perfusion imaging in intermediate to high risk CAD patients, and to provide accurate data of myocardial ischemia at a radiation dose comparable to SPECT MPI.

The encouraging results from this single center study using the 320MDCT are being evaluated in an international, multicenter study with 16 participating hospitals located in eight countries, the CORE320 trial (George et al. 2011; Vavere et al. 2011). This collaborative effort aims to test the accuracy of CTCA in demonstrating ≥50 % coronary artery stenosis and a corresponding perfusion defect on CTP in comparison with (a) QCA-determined ≥50 % stenosis and a corresponding perfusion defect on SPECT MPI, and with (b) QCA-determined ≥50 % stenosis. The study outline is illustrated in Fig. 4.

The study will enroll 400 patients with suspected CAD, who have been referred for coronary catheterization, and who have a research or clinical SPECT MPI performed within 60 days of the coronary catheterization. A research CTCA and CTP will be performed using the protocol outlined in Fig. 2 without the delayed enhanced CT acquisition. The anticipation is that this study will provide sufficient clinical data to evaluate the utility of combined 320MDCT coronary angiography and myocardial perfusion for comprehensive assessment of myocardial viability and ischemia in comparison to established clinical standards which in turn could lead to a change in clinical practice towards the use of 320MDCT as a first line assessment in appropriate patients.

The use of 320MDCT facilitates through-plane temporal homogeneity of image acquisition with a significant reduction in radiation dose and significant improvement in image quality for cardiac CT compared to 64MDCT acquisitions (Torres et al. 2010; Abadi et al. 2011). The utility of performing both anatomical assessment of CAD and functional evaluation of myocardial perfusion is a powerful combination for non-invasive imaging assessment of myocardial viability (Williams et al. 2011; Nasis et al. 2010). It is conceivable that stable patients with a clinical suspicion of CAD and no contraindications to cardiac CT would have an initial CTCA performed at rest. Patients with evaluable coronary artery segments larger than 1.5 mm in diameter and coronary artery stenosis greater than 50 % would require no further imaging, whereas other patients could proceed to have CT myocardial perfusion assessment using vasodilator stress. This combination of imaging with 320MDCT could potentially effectively triage the majority of patients with suspected CAD.

References

Abadi S, Mehrez H, Ursani A, Parker M, Paul N (2011) Direct quantification of breast dose during coronary CT angiography and evaluation of dose reduction strategies AJR 196(2):152–158

Brooks RA, Di Chiro G (1976) Beam hardening in X-ray reconstructive tomography. Phys Med Biol 21(3):390–398

Coyne EP, Belvedere DA, van de Streek PR, Weiland FL, Evans RB, Spaccavento LJ (1991) Thallium-201 scintigraphy after intravenous infusion of adenosine compared with exercise thallium testing in the diagnosis of coronary artery disease. J Am Coll Cardiol 17:1289–1294

Crossett MP, Schneider-Kolsky M, Troupis J (2011) Normal perfusion of the left ventricular myocardium using 320MDCT. JCCT 5:406–411

George RT, Arbab-Zadeh A, Cerci RJ, Vavere AL, Kitagawa K, Dewey M, Rochitte CE, Arai AE, Paul N, Rybicki FJ, Lardo AC, Clouse ME, Lima JA (2011) Diagnostic performance of combined noninvasive coronary angiography and myocardial perfusion imaging using 320-MDCT: the CT angiography and perfusion methods of the CORE320 multicenter multinational diagnostic study. AJR Am J Roentgenol 197(4):829–837

George RT, Arbab-Zadeh A, Miller JM, Kitagawa K, Chang HJ, Bluemke DA et al (2009) Adenosine stress 64- and 256-row detector computed tomography angiography and perfusion imaging: a pilot study evaluating the transmural extent of perfusion abnormalities to predict atherosclerosis causing myocardial ischemia. Circ Cardiovasc Imaging 2:174–182

George RT, Arbab-Zadeh A, Miller JM, Vavere AL, Bengel FM, Lardo AC, Lima JA (2012) Computed tomography myocardial perfusion imaging with 320-row detector CT accurately detects myocardial ischemia in patients with obstructive coronary artery disease. Circ Cardiovasc Imaging 5: 333–340

George RT, Ichihara T, Lima JAC, Lardo AC (2010) A method for reconstructing the arterial input function during helical CT: implications for myocardial perfusion distribution imaging. Radiology 255(2):396–404

George RT, Jerosch-Herold M, Silva C, Kitagawa K, Bluemke DA, Lima JA et al (2007) Quantification of myocardial perfusion using dynamic 64-detector computed tomography. Invest Radiol 42:815–822

George RT, Silva C, Cordeiro MA, di Paula A, Thompson DR, McCarthy WF et al (2006) Multidetector computed tomography

myocardial perfusion imaging during adenosine stress. J Am Coll Cardiol 48:153–160

Gupta NC, Esterbrooks DJ, Hilleman DE, Mohiuddin SM (1992) Comparison of adenosine and exercise thallium-201 single-photon emission computed tomography (SPECT) myocardial perfusion imaging. The GE SPECT Multicenter Adenosine Study Group. J Am Coll Cardiol 19:248–257

Hacker M, Jakobs T, Matthiesen F et al (2005) Comparison of spiral multidetector CT angiography and myocardial perfusion imaging in the noninvasive detection of functionally relevant coronary artery lesions: first clinical experiences. J Nucl Med 46:1294–1300

Kitagawa K, George RT, Arbab-Zadeh A, Lima JAC, Lardo AC (2010) Characterization and correction of beam-hardening artifacts during dynamic volume CT assessment of myocardial perfusion. Radiology 256(1):111–118

Klocke FJ, Baird MG, Lorell BH et al (2003) ACC/AHA/ASNC guidelines for the clinical use of cardiac radionuclide imaging—executive summary: a report of the American College of Cardiology/American Heart Association Task Force on practice guidelines (ACC/AHA/ASNC Committee to revise the 1995 guidelines for the clinical use of cardiac radionuclide imaging). J Am Coll Cardiol 42:1318–1333

Ko B, Cameron J, Defrance T, Seneviratne S (2011) CT stress myocardial perfusion imaging using Multidetector CT—a review. JCCT 5(6):345–356

Ko B, Cameron J, Meredith I, Leung M, Antonis P, Nasis A, Crossett M, Hope S, Lehman S, Troupis J, DeFrance T, Seneviratne S (2012) Computed tomography stress myocardial perfusion imaging in patients considered for revascularization: a comparison with fractional flow reserve. Eur Heart J 33:67–77

Kühl T, Linde J, Fuchs A, Kristensen T, Kelbæk H, George R, Hove J, Kofoed KF (2012) Patterns of myocardial perfusion in humans evaluated with contrast-enhanced 320 multi detector computed tomography. Int J Cardiovasc Imaging 28(7):1739–1747

Lardo AC, Cordeiro MA, Silva C, Amado LC, George RT, Saliaris AP, Schuleri KH, Fernandes VR, Zviman M, Nazarian S, Halperin HR, Wu KC, Hare JH, Lima JAC (2006) Contrast enhanced multidetector computed tomography viability imaging following myocardial infarction: characterization of myocyte death, microvascular obstruction and chronic scar. Circulation 113:394–404

Mehra V, Ambrose M, Valdiviezo-Schlomp C, Schuleri K, Lardo AC, Lima JA, George RT (2011a) CT-based myocardial perfusion imaging-practical considerations: acquisition, image analysis, interpretation, and challenges. J Cardiovasc Transl Res 4(4): 437–448

Mehra V, Valdiviezo C, Arbab-Zadeh A, Ko B, Seneviratne S, Cerci R, Lima J, George R (2011b) A stepwise approach to the visual interpretation of CT-based myocardial perfusion. JCCT 5(6): 357–369

Nasis A, Seneviratne S, DeFrance T (2010) Advances in contrast-enhanced cardiovascular CT for the evaluation of myocardial perfusion. Curr Cardiovasc Imaging Rep 3:372–381

Nguyen T, Heo J, Ogilby JD, Iskandrian AS (1990) Single photon emission computed tomography with thallium-201 during adenosine-induced coronary hyperemia: correlation with coronary arteriography, exercise thallium imaging and two-dimensional echocardiography. J Am Coll Cardiol 16:1375–1383

Nishimura S, Mahmarian JJ, Boyce TM, Verani MS (1992) Equivalence between adenosine and exercise thallium-201 myocardial tomography: a multicenter, prospective, crossover trial. J Am Coll Cardiol 20:265–275

Olson EA, Han KS, Pisano DJ (1981) CT reprojection polychromaticity correction for three attenuators. IEEE Trans Nucl Sci 28(4): 3628–3640

Parodi O, Marcassa C, Casucci R et al (1991) Accuracy and safety of technetium-99 m hexakis 2-methoxy-2-isobutyl isonitrile (sestamibi) myocardial scintigraphy with high dose dipyridamole test in patients with effort angina pectoris: a multicenter study. Italian Group of Nuclear Cardiology. J Am Coll Cardiol 18:1439–1444

Pijls NH, de Bruyne B, Peels K, van der Voort PH, Bonnier HJ, Bartunek JKJJ, Koolen JJ (1996) Measurement of fractional flow reserve to assess the functional severity of coronary-artery stenoses. N Engl J Med 334:1703–1708

Rumberger JA, Bell MR (1992) Measurement of myocardial perfusion and cardiac output using intravenous injection methods by ultrafast (cine) computed tomography. Invest Radiol 27:S40–S46

Rumberger JA, Feiring AJ, Lipton MJ, Higgins CB, Ell SR, Marcus ML (1987) Use of ultrafast computed tomography to quantitate regional myocardial perfusion: A preliminary report. J Am Coll Cardiol 9:59–69

Schuijf JD, Wijns W, Jukema JW, Atsma DE, de Roos A, Lamb HJ, Stokkel MPM, Dibbets-Schneider P, Decramer I, De Bondt P, van der Wall EE, Vanhoenacker PK, Bax JJ (2006) Relationship between noninvasive coronary angiography with multi-slice computed tomography and myocardial perfusion imaging. J Am Coll Cardiol 48(12):2508–2514

Torres F, Crean A, Nguyen ET, Doyle D, Menezes R, Ayyappan AP, Abadi S, Paul N (2010) Abolition of respiratory motion artifact in CT coronary angiography with ultrafast examinations: a comparison between 64-row and 320-row multidetector scanners. Can Assoc Radiol J 61:5–12

Valdiviezo C, Ambrose M, Mehra V, Lardo AC, Lima JAC, George RT (2010) Quantitative and qualitative analysis and interpretation of CT perfusion imaging. J Nucl Cardiol 17:1091–1100

Vavere AL, Simon GG, Lima JAC (2011) Diagnostic performance of combined noninvasive coronary angiography and myocardial perfusion imaging using 320 row detector computed tomography: design and implementation of the CORE320 multicenter, multinational diagnostic study. JCCT 5:370–381

Williams M, Reid J, McKillop G, Weir N, van Beek E, Uren N, Newby D (2011) Cardiac and coronary CT. Comprehensive imaging approach in the assessment of coronary heart disease. Heart 97:1198–1205

Zatz LM, Alvarez RE (1977) An inaccuracy in computed tomography: the energy dependence of CT values. Radiology 124(1):91–97